ACS APPLIED MATERIALS & INTERFACES

RESEARCH ARTICLE

www.acsami.org

Low-Temperature Approach to High-Yield and Reproducible Syntheses of High-Quality Small-Sized PbSe Colloidal Nanocrystals for Photovoltaic Applications

Jianying Ouyang,[†] Carl Schuurmans,[†] Yanguang Zhang,[‡] Robbert Nagelkerke,[†] Xiaohua Wu,[‡] David Kingston,[§] Zhi Yuan Wang,[⊥] Diana Wilkinson,[¶] Chunsheng Li,[∥] Donald M. Leek,[†] Ye Tao,[‡] and Kui Yu*[,†]

[†]Steacie Institute for Molecular Sciences, [‡]Institute for Microstructural Sciences, and [§]Institute for Chemical Process and Environmental Technology, National Research Council of Canada, Ottawa, Ontario K1A 0R6, Canada

[⊥]Department of Chemistry, Carleton University, 1125 Colonel By Drive, Ottawa, Ontario K1S 5B6, Canada

[¶]Defence Research and Development Canada, 3701 Carling Avenue, Ottawa, Ontario K1A 0Z4, Canada

[∥]Healthy Environment and Consumer Safety Branch, Health Canada, Ottawa, Ontario K1A 1C1, Canada

Supporting Information

ABSTRACT: Small-sized PbSe nanocrystals (NCs) were synthesized at low temperature such as 50−80 °C with high reaction yield (up to 100%), high quality, and high synthetic reproducibility, via a noninjection-based one-pot approach. These small-sized PbSe NCs with their first excitonic absorption in wavelength shorter than 1200 nm (corresponding to size < ∼3.7 nm) were developed for photovoltaic applications requiring a large quantity of materials. These colloidal PbSe NCs, also called quantum dots, are high-quality, in terms of narrow size distribution with a typical standard deviation of ∼7−9%, excellent optical properties with high quantum yield of ∼50−90% and small full width at half-maximum of ∼130−150 nm of their band-gap photoemission peaks, and high storage stability. Our synthetic design aimed at promotion of the formation of PbSe monomers for fast and sizable nucleation with the presence of a large number of nuclei at low temperature. For formation of the PbSe monomer, our low-temperature approach suggests the existence of two pathways of Pb−Se (route a) and Pb−P (route b) complexes. Either pathway may dominate, depending on the method used and its experimental conditions. Experimentally, a reducing/nucleation agent, diphenylphosphine, was added to enhance route b. The present study addresses two challenging issues in the NC community, the monomer formation mechanism and the reproducible syntheses of small-sized NCs with high yield and high quality and large-scale capability, bringing insight to the fundamental understanding of optimization of the NC yield and quality via control of the precursor complex reactivity and thus nucleation/growth. Such advances in colloidal science should, in turn, promote the development of next-generation low-cost and high-efficiency solar cells. Schottky-type solar cells using our PbSe NCs as the active material have achieved the highest power conversion efficiency of 2.82%, in comparison with the same type of solar cells using other PbSe NCs, under Air Mass 1.5 global (AM 1.5G) irradiation of 100 mW/cm^2.

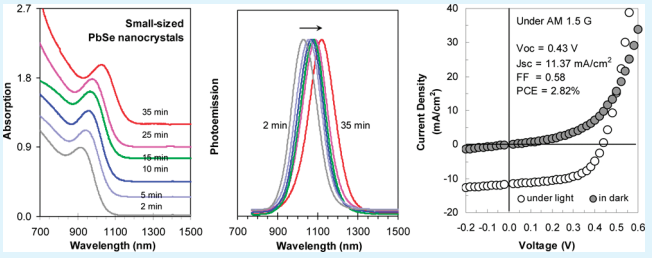

KEYWORDS: formation mechanism, monomer, nucleation/growth, reducing agent, small-sized PbSe nanocrystals, quantum dots, high particle/reaction yield, photovoltaics

INTRODUCTION

Lead-based quantum dots (QDs) are important infrared (IR)-active materials in various applications such as in photovoltaic (PV) devices.[1] Semiconductor lead selenide (PbSe) is of particular appeal, with its bulk band gap in the mid-IR (0.26 eV) and large exciton Bohr radius of 46 nm, rendering extremely strong quantum confinement to its nanosized structures.[2] Accordingly, colloidal PbSe QDs can be engineered to absorb and emit in a vast spectral range, spanning from ∼800 to 4000 nm with high photoluminescence (PL) emission quantum yields (QYs).[3−8] Hence, PbSe QDs are important materials for near-IR (NIR; >700 nm) and mid-IR (>2500 nm) applications, including biological imaging/labeling,[9,10] solar cells,[11−16] light-emitting devices,[17] and telecommunications.[18,19] PbSe nanocrystals (NCs) are especially attractive in the PV application, with a multiple exciton generation effect reported.[20−23] The PbSe-based solar cells may exhibit power conversion efficiencies (PCEs) exceeding the Shockley−Queisser theoretical limit of 33.7%.[24]

Received: November 17, 2010
Accepted: December 7, 2010
Published: January 18, 2011

Small-sized PbSe NCs are in outstanding demand as active materials in solar cell devices. For example, solar cell devices made from large PbSe NCs (>∼3.8 nm) showed no appreciable PV effect, whereas those made from small PbSe NCs (<∼3.8 nm) exhibited increasing open-circuit voltage (V_{oc}) with decreasing NC size.[14] Also, the optimal band-gap wavelength was calculated to be in the range of ∼900−1300 nm, with the maximum thermodynamic conversion efficiencies of PV devices operated at ∼1100 nm (band-gap energy E_g ∼ 1.1 eV).[16] It is worth noting that the size of the PbSe NCs with the first excitonic absorption peak at ∼1000 nm was described as 2.4 nm,[25] while 3.0 nm is estimated according to the relationship reported on the absorption peak position and size.[26] At present, it is still challenging to accurately obtain the size information of small NCs.[27−29] Accordingly, for small-sized NCs, the use of their first excitonic absorption peak positions instead of their sizes can be practical to minimize the confusion in the size determination.[5]

The first synthesis of colloidal PbSe QDs was reported in 2001 with a hot-injection approach.[3] Since then, a number of modified synthetic conditions have been reported.[3−8] Usually, Pb and Se precursors were lead oleate [$Pb(oleate)_2$ or $Pb(OA)_2$] and *n*-trioctylphosphine selenide (TOPSe), respectively, with excess feed of TOPSe over $Pb(OA)_2$ and 1-octadecene (ODE) as the solvent. The injection/growth temperature was in the range of 80−250 °C, with the growth periods of 10 s to 10 min depending on the desired sizes. These reactions can be described as method (1) and represented by the hot-injection equation (eq 1a).

$$Pb(oleate)_2 + TOPSe \xrightarrow{ODE} PbSe\ QDs \quad (hot\ injection) \quad (1a)$$

Method (1) could efficiently produce large-sized PbSe QDs with the first excitonic absorption peak position longer than 1300 nm but was ineffective in producing small-sized PbSe QDs with the first excitonic absorption peak position shorter than 1200 nm (corresponding to size <∼3.7 nm). It has been acknowledged that one of the serious limitations of method (1) is low chemical/reaction/conversion yields or particle yield (in terms of NC concentration or the number of particles formed),[5,25] particularly for small-sized PbSe.

The use of diphenylphosphine (DPP) and 1,2-hexadecanediol (HDD) in the synthesis of PbSe NCs was documented; however, with the assistance of DPP or HDD, the two hot-injection conditions explored were not able to produce small-sized PbSe NCs with high yield.[25,30] For example, PbSe NCs with the first excitonic absorption peak at ∼1000 nm were obtained at 10 s/160 °C with only 5% chemical yield,[25] as shown in Table 1. Very recently, Krauss and co-workers reported that pure tertiary phosphine selenide such as TOPSe did not react with $Pb(OA)_2$, but secondary phosphine selenide $Se{=}PH(R_a)_2$ did.[31] The authors also commented that control of the QD sizes with pure secondary phosphine selenide was not well understood. The active impurities in commercially available *n*-trioctylphosphine (TOP) and *n*-tributylphosphine (TBP) are dioctylphosphine (DOP) and dibutylphosphine (DBP), respectively.

Compared to the hot-injection approach, a noninjection approach features easy handling with high synthetic reproducibility and large-scale production capability. With the one-pot noninjection approach, we have successfully developed various high-quality colloidal QDs, including regular[32−34] and magic-sized QDs.[27−29,35−37] Herein, we report on our development of a low-temperature noninjection one-pot approach to prepare small-sized PbSe NCs with high chemical yield and high quality, aiming at their potential in PV devices. It is conceivable that the presence of a large number of nuclei and long growth periods should favor formation of the desired PbSe NCs. To achieve sizable nucleation, the reactivity of precursors and the degree/rate of supersaturation of the monomer should be high, the latter of which could be facilitated by a low growth temperature. In order to promote the monomer formation and understand the mechanisms proposed on the monomer formation,[25,30,31] we designed five methods using commercially available TOP (90%), TBP (97%), and DPP (98%) without purification. Experimentally, the low-temperature realization of high-quality small-sized NCs with high reaction yield (up to 100%) was achieved via the presence of a strong reducing/nucleation agent DPP. Besides, this study importantly addresses another essential issue in QD science and technology: the formation mechanism of monomers. A modified mechanism is proposed for our low-temperature (50−80 °C) approach to small-sized PbSe QDs: there are two pathways via Pb−Se (route a) and Pb−P (route b) complexes, respectively; the latter may not involve the formation of Pb^0.[25,30,31] Depending on the method and

Table 1. Summary of the Particle Yields of Our Small-Sized PbSe NCs Obtained from the Five Low-Temperature Noninjection Methods Represented by Equations 1−5 and the Corresponding Chemical Yields and the Numbers of Particles, Together with the Available Literature Data[25,30]

method	batch	growth period (min)/temp (°C)	feed molar ratio	abs PP (nm), as synthesized	[PbSe] (μmol/kg)	chemical yield (%)	no. of NCs[a]
1	Figure 4, batch no. TBP	35/80	1:2.5 Pb-to-TOPSe	1181	2.6	1.1	1.79×10^{16}
2	Figure 2, batch a	35/50	1:2.5 Pb-to-TOPSe	1045	111.0	30.0	7.84×10^{17}
2	Figure 2, batch b	25/60	1:2.5 Pb-to-TOPSe	1156	85.2	33.1	6.06×10^{17}
2	Figure 3, batch 1 DPP	5/80	4:1 Pb-to-TOPSe	1157	196.7	85.4	1.52×10^{18}
2	Figure 3, batch 1 DPP	10/80	4:1 Pb-to-TOPSe	1239	193.3	100	1.49×10^{18}
3	Figure 4, batch 1.6 TBP	35/80	1:2.5 Pb-to-TOPSe	1145	10.1	3.7	6.75×10^{16}
4	Figure 5, batch b	35/80	1:2.5 Pb-to-TBPSe	1024	16.9	4.3	1.16×10^{17}
5	Figure 2, batch c	35/50	1:2.5 Pb-to-TBPSe	1156	95.2	37.0	6.56×10^{17}
1	ref30, 0 DPP−1 Pb	2/135	1:5 Pb-to-TOPSe	1358		2.3	1.81×10^{16}
2	ref30, 0.08 DPP−1 Pb	2/135	1:5 Pb-to-TOPSe	1736		11.6	3.09×10^{16}
2	ref30, 0.15 DPP−1 Pb	2/135	1:5 Pb-to-TOPSe	1716		16.2	4.53×10^{16}
2[b]	ref25, 4 HDD−1 Pb	10 s/160	1:2 Pb-to-TOPSe	1000		5	
2[b]	ref25, 4 HDD−1 Pb	50/160	1:2 Pb-to-TOPSe	1498		16	

[a] Normalized to 1 mmol of feed $Pb(OA)_2$ or Se, which was the limiting agent in a reaction. [b] Route b was realized with HDD via a Pb−O complex. The lower cost of $Pb(OA)_2$ than that of TOPSe is worth noting.

its experimental conditions, either pathway can dominate. The present synthetic development brings insight to the fundamental understanding of the monomer formation mechanism and the experimental parameters controlling such monomer formation and thus sizable nucleation. Using our PbSe NCs as the active material, the PCE has reached a new record of 2.82% from the previous 2.1% reported for the same PbSe NC-based Schottky-type solar cells. [14]

RESULTS AND DISCUSSION

The present study focuses on the development of a low-temperature noninjection one-pot synthetic protocol for the reproducible preparation of small-sized PbSe NCs with high particle yield and high quality, suitable for solar cell applications. To the best of our knowledge, the present study is the first using a noninjection-based approach to produce PbSe NCs. First, our noninjection approach adapted the "traditional" method (1) shown by eq 1. Typically, a reaction was carried out in ODE, with $Pb(OA)_2$ and TOPSe as Pb and Se precursors, respectively. Under our synthetic condition with a feed molar ratio of 1:2.5 Pb-to-Se and a Pb concentration of ~66 mmol/L, the nucleation took place at ~80 °C. The onset of nucleation is inferred at the color change of a reaction from colorless to light brownish.

To promote formation of the monomer with nucleation at lower temperature and formation of a large number of nuclei, we chose to explore the influence of DPP and/or TBP. Therefore, we investigated the five methods shown by eqs 1−5. Methods (3)−(5) have not been reported before and are thus new, while the experimental conditions used for methods (1) and (2) were different from those reported.[3−8,25,30,31]

$$Pb(oleate)_2 + TOPSe/TOP \xrightarrow{ODE} PbSe\ QDs \quad (1)$$

$$Pb(oleate)_2 + TOPSe/TOP + DPP \xrightarrow{ODE} PbSe\ QDs \quad (2)$$

$$Pb(oleate)_2 + TOPSe/TOP + TBP \xrightarrow{ODE} PbSe\ QDs \quad (3)$$

$$Pb(oleate)_2 + TBPSe/TBP \xrightarrow{ODE} PbSe\ QDs \quad (4)$$

$$Pb(oleate)_2 + TBPSe/TBP + DPP \xrightarrow{ODE} PbSe\ QDs \quad (5)$$

Methods (2) and (5) represent the use of DPP to inspire nucleation and growth of the PbSe QDs. In the presence of DPP, the nucleation could be activated at temperature as low as ~40 °C. With a small amount of DPP added (such as with feed molar ratios of 1.47:1 DPP-to-Pb and 1:2.5 Pb-to-Se), small-sized PbSe QDs could be obtained at 50−60 °C with a very high nucleation rate and an enhanced particle yield by a factor of ~40−50 when DOPSe/TOPSe (DOPSe represents the active compound in an ~1.0 M TOPSe stock solution) was used as the Se precursor as shown by eq 2 and that by a factor of ~4 when DBPSe/TBPSe (DBPSe represents the active compound in an ~1.8 M TBPSe stock solution) was used as the Se precursor as shown by eq 5. It is amazing that, with a feed molar ratio of 4:1 Pb-to-TOPSe, the presence of DPP in our noninjection approach led to small-sized PbSe NCs with nearly 100% yield (see Table 1), demonstrating excellent control of nucleation and growth via promotion of route b. Under such a condition but without DPP, nucleation and growth was much less successful. The resulting PbSe NCs with high particle yield exhibited optical properties (including PL QYs) comparable to those with low particle yield obtained in the absence of DPP. Note that, compared to those reported,[25,30] the different experimental parameters including the Pb-to-Se feed molar ratio and growth temperature were used in method (2), in order to promote the high particle yield together with the high quality of the small-sized PbSe NCs.

Methods (3) and (4) represent the use of TBP to promote nucleation and growth of the PbSe NCs. As shown by eq 3, TBP was added to the reaction mixture [method (1)], resulting in an increase of the particle yield by a factor of ~3. The nucleation seemed to occur at ~65 °C; accordingly, the growth was carried out at low temperature such as 60−80 °C. Here, DBP/TBP acted as a reducing agent but was stronger than DOP/TOP, which might be explained by the relatively small steric hindrance of the Pb−P complex $(OA)_2Pb-PH(C_4H_9)_2$ or $(OA)_2Pb-P(C_4H_9)_3$ compared to that of $(OA)_2Pb-PH(C_8H_{17})_2$ or $(OA)_2Pb-P(C_8H_{17})_3$. As shown by eq 4, DBPSe/TBPSe was used to replace DOPSe/TOPSe [method (1)], resulting in a significant increase of the particle yield by a factor of ~8. The nucleation seemed to take place at ~50 °C, and the growth in size at 60−80 °C was slowed because of the fact that the available monomer for further growth was limited in the presence of a large amount of nuclei. Here, the reactivity of DBPSe seems to be higher than that of DOPSe, leading to the presence of more nuclei at lower temperature, which might be explained by the relatively small steric hindrance of the Pb−Se complex $(OA)_2Pb-Se{=}PH(C_4H_9)_2$ compared to that of $(OA)_2Pb-Se{=}PH(C_8H_{17})_2$. Here, the presence of TBP [method (3)] or the use TBPSe instead of TOPSe [method (4)] promoted the particle yield, while method (4) was more efficient. The resulting small-sized PbSe QDs exhibited narrow size distribution with a typical standard deviation of ~7% and high PL QYs (~70−90%) as referenced to IR 26 (lit. QY ~ 0.5% in dichloroethane).[38]

Note that the formation mechanism of the monomer is very much fundamental; its understanding is critical to designing and optimizing experimental methods and conditions to control the kinetics of monomer formation and thus the resulting nucleation for the reproducible syntheses of QDs with high yield and desired sizes. On the basis of our experimental observations from methods (1)−(5) carried out at low temperature and those proposed,[25,30,31] we propose that formation of the PbSe monomer involves two routes via Pb−Se and/or Pb−P complexes, respectively. The two complexes may occur simultaneously; however, whether route a or b dominates depending on the method and experimental conditions.

Particularly, for method (2), we propose that route a experienced formation of a Pb−Se complex as shown by eq aM, while route b experienced formation of a Pb−P complex as shown by eq bM. Route b dominated.

$$(oleate)_2Pb + DOPSe \rightarrow Pb-Se\ complex \rightarrow PbSe\ monomer \quad [method\ (2)] \quad (aM)$$

$$(oleate)_2Pb + DPP \rightarrow Pb-P\ complex \rightarrow PbSe\ monomer \quad [method\ (2)] \quad (bM)$$

The reactivity of secondary phosphine selenide was much higher than that of tertiary phosphine selenide;[31] however, formation of the former seemed to be more difficult than that of the latter.[31] Moreover, under our experimental conditions of method (2), no formation of DPPSe was detected by ^{31}P NMR when DPP was mixed with TOPSe/TOP even after 3 h at 80 °C, as shown in Scheme S1 in the Supporting Information (SI).

In order to compare these low-temperature noninjection methods (represented by eqs 1−5), as well as the literature-reported

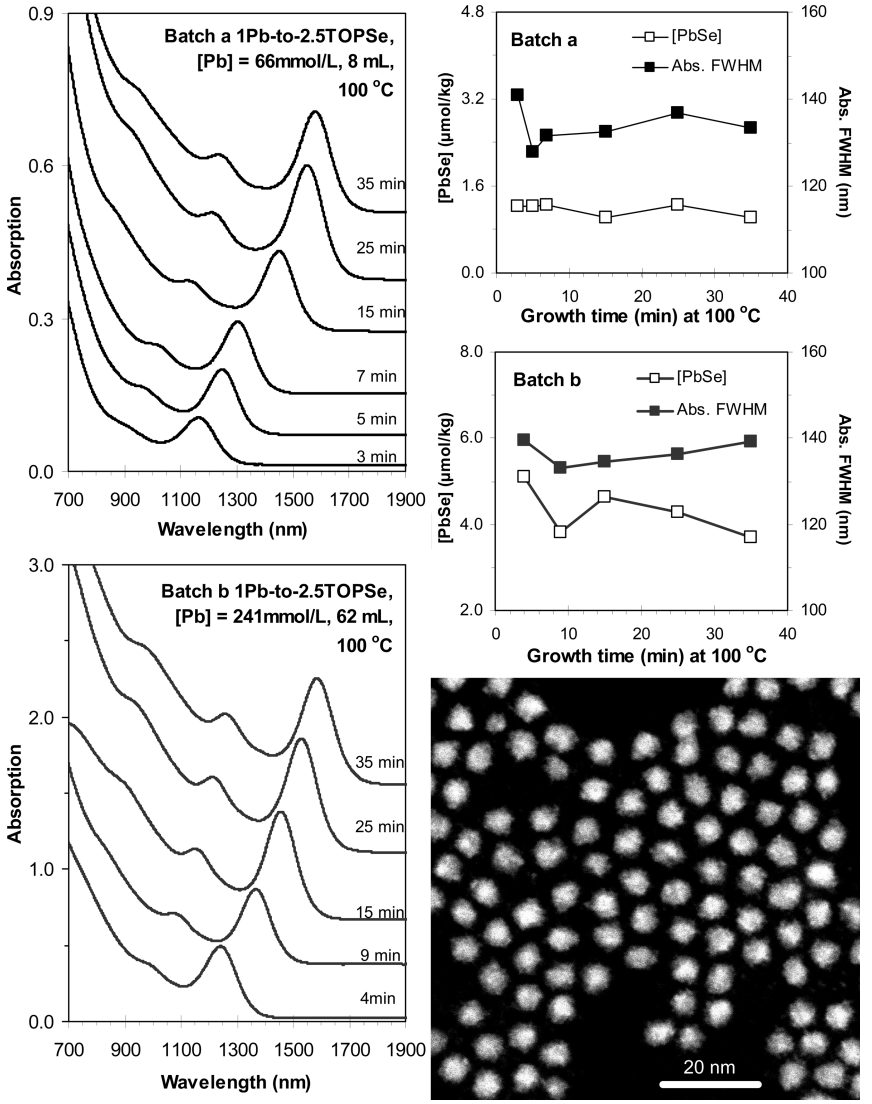

Figure 1. Temporal evolution of absorption (offset) of the PbSe NCs from batches a (left top) and b (left bottom), with the feed molar ratio of 1:2.5 Pb-to-TOPSe. The [Pb] and volume of the reaction media are indicated, together with the growth temperature and periods. Batch b is ∼28-fold scale of batch a. The absorption spectra were normalized to 1.0 g of crude growth mixtures sampled and dispersed in 1.0 mL of TCE. The nanocrystal concentration [PbSe] in μmol/kg in crude growth mixtures (left y axis) and absorption fwhm in nm (right y axis) from batches a (right top) and b (right middle) are summarized. (Right bottom) Typical high-angle annular dark field scanning transmission electron microscopy image of the PbSe NCs prepared from batch b with a growth period of 25 min. The mean size was measured to be ∼5.0 nm with a standard deviation of ∼7%.

high-temperature hot-injection methods, the particle yields of our small-sized PbSe NCs obtained are summarized in Table 1, together with the corresponding chemical yields and numbers of particles. The available literature data are also summarized.[25,30] It is noteworthy that our low-temperature method (2) approach could produce ∼100 times more NCs (in number) than the reported approach did.[30] To describe a synthetic approach to NCs, particularly small-sized NCs, the use of particle yields or particle numbers seems to be more suitable than that of chemical/reaction/conversion yields. Note that the present mechanism proposed for the PbSe monomer formation should be suitable for other QD systems such as IV−VI, II−V, and II−VI; furthermore, route b could be promoted by various chemicals including phosphines and diols.[25] For example, formation of a Cd−P complex was proposed on the formation of CdSe magic-sized QD Family 408.[37]

Accordingly, the syntheses of small-sized PbSe QDs from the five low-temperature noninjection methods are presented, mainly, in the following order: first, method (1) in the absence of DPP and TBP (eq 1), second, method (2) in the presence of DPP and the use of DOPSe/TOPSe (eq 2) and method (5) in the presence of DPP and the use of DBPSe/TBPSe (eq 5), and, third, method (3) in the presence of TBP and the use of DOPSe/TOPSe (eq 3) and method (4) and the use of DBPSe/TBPSe (eq 4). The development of the small-sized PbSe QDs aims at the PV application; thus, finally one example of a solar cell device with 2.82% PCE fabricated with our small-sized PbSe QDs is presented.

Figure 1 addresses method (1), the noninjection-based synthesis of PbSe NCs with TOPSe/TOP as the Se precursor, without any additional reducing agents. The synthetic batch a started with feed molar ratios of 1:2.5 Pb-to-Se and a Pb concentration of 66 mmol/L; the reaction medium was ∼8 mL, mainly consisting of ODE with 18% TOP (by volume). The growth was carried out at 100 °C. The PbSe NCs grew in size as monitored from 3 to

35 min. Their first excitonic absorption peaks red-shifted from 1162 to 1577 nm, corresponding to an increase in size from ~3.6 to ~5.1 nm.[26] The absorption full width at half-maximum (fwhm; Gaussian-fitted) was ~130−140 nm, and the particle number was low with the NC concentration [PbSe] in the reaction medium of ~1.0−1.2 μmol/kg and the chemical yield of ~1.1−2.8% (similar to that reported in 2006 and shown in Table 1).[30] [PbSe] was determined by Lambert−Beer's law, $A = \varepsilon CL$, where the molar extinction coefficient ε was estimated from the PbSe NCs size and corrected by the size distribution (see the Experimental Methods section for details).[26]

Our noninjection-based approach features ready large-scale capability and high synthetic reproducibility, leading to PbSe NCs with high quality. As shown in Figure 1, batch b, a ~28-fold scale-up synthesis (from 66 to 241 mmol/L and from 8 to 64 mL) also led to high-quality PbSe NCs, as demonstrated by their narrow absorption fwhm. The typical size standard deviation is ~7% for the 25-min sample from batch b, as shown by transmission electron microscopy (TEM) in Figures 1 and S1A in the SI. Similar chemical yields of 1.6−2.9% were obtained. Accordingly, our noninjection synthesis could produce PbSe NCs with qualities comparable to those of the best reported hot-injection products.[5,26]

The preparation of TOPSe involved the use of TOP and Se with a 2.2:1 TOP-to-Se feed molar ratio. Thus, the presence of TOPSe is associated with the presence of DOPSe and free TOP/DOP. TOP was reported to be a weak reducing agent; TOP reduces $Pb(OA)_2$ but in a much more subtle manner compared to DPP.[30] Accordingly, it is easy to understand that 1:(2−5) Pb-to-TOPSe feed molar ratios were usually used to prepare PbSe NCs.[3−8,25,30] For promotion of the monomer formation, the effects of the Pb-to-TOPSe feed molar ratio and the TOP amount should be considered in our low-temperature approach method (1). The effect of the Pb-to-Se feed molar ratio is shown in Figure S1B in the SI: the lower the Pb-to-TOPSe feed molar ratio, the faster the nucleation, in conjunction with the higher the particle number and the narrower the size distribution. Such an effect of the Pb-to-TOPSe feed molar ratio on the nucleation/growth rate and NC quality can be explained: the lower the Pb-to-TOPSe feed molar ratio used, the more DOPSe/TOPSe and TOP that is present and the more efficient route a becomes. Meanwhile, $Pb(OA)_2$ is highly viscous (crystallized below 30 °C); the presence of a large amount of $Pb(OA)_2$ may hinder nucleation/growth because of the difficulty of diffusion.

The effect of the TOP amount on formation of the PbSe NCs was explored and is presented in Figure S1C in the SI, with a feed molar ratio of 1.5:1 Pb-to-TOPSe and [Se] of 150 mmol/L. When the TOP amount was only 14% (v/v), the nucleation/growth took place slowly, leading to PbSe NCs exhibiting absorption fwhm of 174 nm with an extremely low [PbSe] of ~0.5 μmol/kg. When the TOP amount was 65% (v/v), the nucleation/growth was much faster, leading to PbSe NCs exhibiting an absorption fwhm of 147 nm with [PbSe] of ~2.9 μmol/kg. When the TOP amount was 90% (v/v), the nucleation (which might occur at ~40−50 °C) was the fastest, leading to PbSe NCs exhibiting an absorption fwhm of 229 nm with [PbSe] of ~5.7 μmol/kg. The growth in batch TOP 90% (v/v) was restricted by a limited monomer concentration due to a large consumption for formation of a high number of nuclei. Consequently, the larger the TOP amount, the more the DOP, the more the monomer (via route b), the faster the nucleation/growth, and the higher the particle number. Interestingly, such a TOP effect is less recognized for synthesis with a small $Pb(OA)_2$-to-TOPSe feed molar ratio. For instance, when the feed molar ratio was 1:2.5 Pb-to-Se, as shown in Figure 1, the resulting PbSe NCs from the two batches with 18% and 61% TOP (v/v) exhibited similarity in both quality and [PbSe]. Therefore, the effect of the TOP amount was more pronounced with a feed molar ratio of 1.5:1 Pb-to-Se than with 1:2.5 Pb-to-Se; the former exhibited slower nucleation/growth than the latter (as shown in Figure S1B in the SI). Such knowledge was helpful in guiding us in the design of method (2), in the presence of DPP with batches with high Pb-to-TOPSe feed molar ratios.

Figures 1 and S1 in the SI show that method (1) with the present noninjection approach is excellent for producing PbSe NCs but is not efficient enough to produce small-sized PbSe NCs [even with a thorough exploration of the experimental conditions such as with (4−1):(1−2.5) Pb-to-Se feed molar ratios and with TOP addition]. Subsequently, we investigated the presence of DPP and/or TBP assisting with the formation of small-sized PbSe NCs with high yield and high quality.

Now, let us turn our attention to the effect of the use of DPP [methods (2) and (5)] on the formation of small-sized PbSe NCs with high yield and quality. Figure 2 shows the temporal evolution of the absorption (offset) and emission (normalized) of the PbSe NCs sampled from three batches with feed molar ratios of 1.47:1 DPP-to-Pb, 2.2:1 OA-to-Pb, and 1:2.5 Pb-to-Se and [Pb] ~ 71 mmol/L. The Se precursor and growth temperature were TOPSe and 50 °C [batch a, method (2)], TOPSe and 60 °C [batch b, method (2)], and TBPSe and 50 °C [batch c, method (5)]. For the three batches, it seemed that nucleation took place at ~40 °C.

For batch a, the growth of PbSe NCs was relatively slow. They exhibited a red shift of their absorption peak positions from 853 to 1084 nm, during the growth period of 2−45 min at 50 °C, a red shift of their emission from 1009 to 1189 nm, and a continuous increase of the emission fwhm from 148 to 175 nm. Meanwhile, [PbSe] increased from ~120 to ~145 μmol/kg in the first 10 min, followed by a continuous decrease to ~111 μmol/kg at 35 min and to ~109 μmol/kg at 45 min. The chemical yields were ~30% at 30 min and ~33% at 45 min. Here, the decrease of the particle yield and the increase of the chemical yield are worth noting. For the 35-min growth ensemble, its absorption peak position, [PbSe], chemical yield, and number of particles are presented in Table 1. The PL QY was in range of ~50−60%.

For batch b, the growth was faster than that of batch a. The PbSe NCs exhibited a red shift of their absorption peak positions from 807 to 1278 nm, during the growth period of 2−45 min at 60 °C, a red shift of their emission from 959 to 1342 nm, and a continuous increase of the emission fwhm from 148 to 171 nm. Meanwhile, [PbSe] decreased sharply from ~153 to ~98 μmol/kg in the first 5 min, followed by a further decrease to ~85 μmol/kg at both 25 and 45 min. The chemical yields were ~33% at 25 min and ~45% at 45 min. The 25-min growth ensemble exhibited the same absorption peak position as the 35-min growth ensemble of batch c; thus, its relevant data are summarized in Table 1. It seems that a ripening similar to that of batch c took place. The PL QY was in the range of ~30−80%, the value of which is similar to that of batch c but higher than that of the PbSe NCs synthesized under similar conditions but without DPP [as shown in Figure 5a, method (1)]. Accordingly, our experimental results suggested that the use of DPP might not lead to a decrease of the PL QY (25%). Sophisticated tuning of the

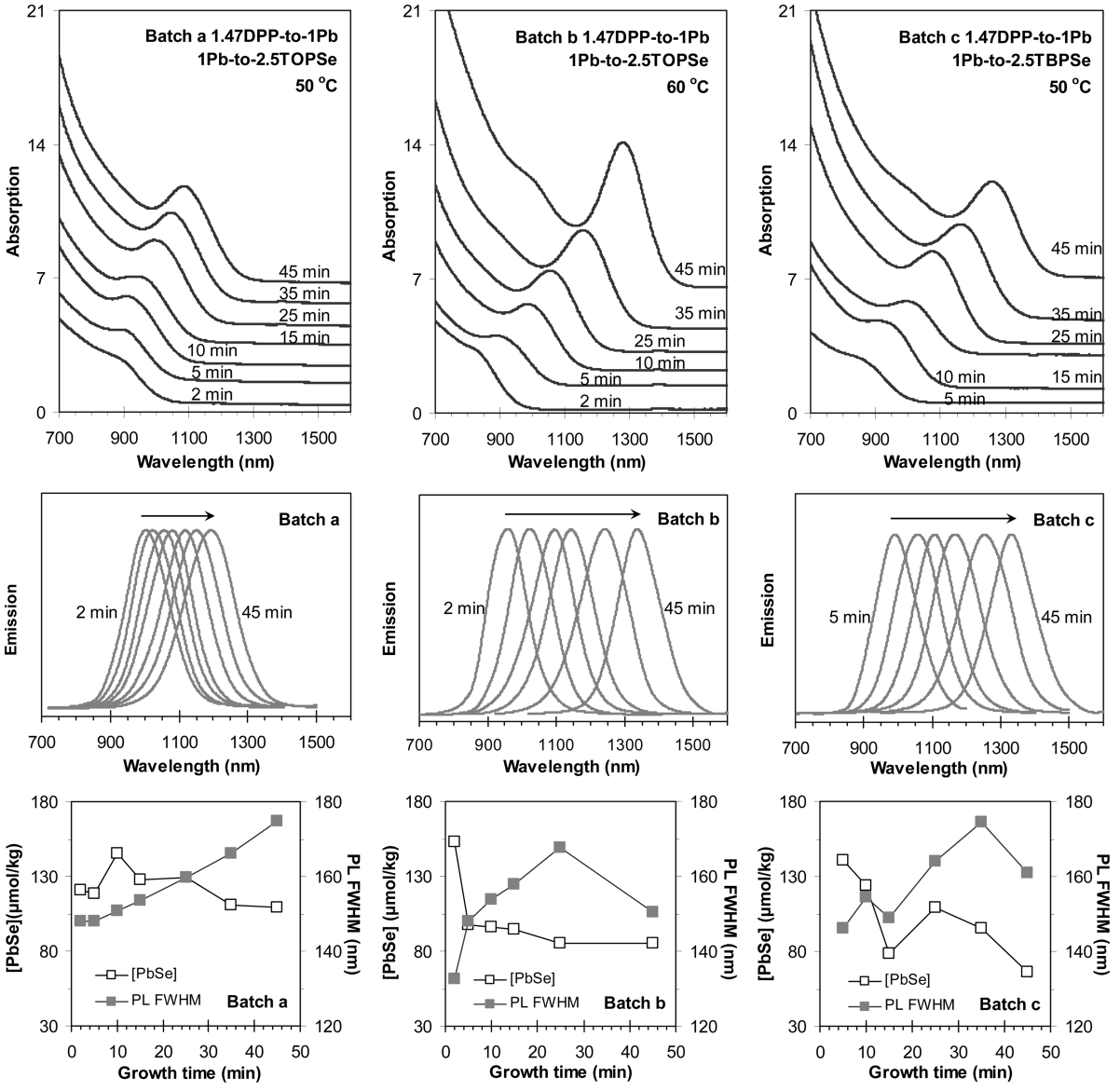

Figure 2. Investigation of the effect of the presence of DPP on the formation of PbSe NCs. The NCs were synthesized from three batches with a feed molar ratio of 1:2.5 Pb-to-Se and [Pb] ~ 71 mmol/L. The Se precursors used, together with the growth temperature and periods, are indicated. The temporal evolution of the absorption (upper panel, offset), emission (middle panel, normalized), and [PbSe] in μmol/kg (lower panel, left y axis) and PL fwhm in nm (lower panel, right y axis) of the PbSe NCs from the three batches with the Se precursor of TOPSe (at 50 °C growth temperature), batch a, TOPSe (at 60 °C growth), batch b, and TBPSe (at 50 °C growth), batch c. The absorption spectra were normalized to 1.0 g of crude reaction mixtures in 1.0 mL of TCE. The PL emission spectra were normalized; diluted sample dispersions in TCE were used for the PL emission measurements with absorbance at the excitation wavelength ~0.1.

synthetic parameters in order to achieve balanced nucleation/growth is outstandingly demanded.

For batch c, the PbSe NCs exhibited a red shift of their absorption peak positions from 822 to 1257 nm, during the growth period of 5−45 min at 50 °C, a red shift of their emission peak positions from 996 to 1334 nm, a decrease of [PbSe] continuously from ~141 to ~66 μmol/kg, and an increase of the PL fwhm progressively from 146 to 174 nm. The chemical yields at 25−45 min growth were ~32−37%. Also, the relevant data for the 35-min growth ensemble are shown in Table 1. It seems that ripening took place. The PL QY was in the range of ~50−75%, the value of which is lower than that of the PbSe NCs synthesized under similar conditions but without DPP [as shown in Figure 5b, method (4)].

Note that the amount of DPP used is an important parameter. Another batch was studied with a 4.4:1 DPP-to-Pb feed molar ratio and otherwise the same conditions as those of batch b (of Figure 2). The temporal evolution of absorption of the PbSe NCs from this 4.4:1 DPP-to-Pb batch is shown in Figure S2 in the SI. Compared to batch b 1.47:1 DPP-to-Pb, the PbSe NCs from batch 4.4:1 DPP-to-Pb red-shifted relatively fast, with an average value of ~99 μmol/kg of [PbSe].

As aforementioned for method (1), nucleation (at 80 °C) was much more difficult for batches with high Pb-to-TOPSe feed molar ratios than for batches with low Pb-to-TOPSe feed molar ratios, as shown in Figure S1B in the SI. DPP is a strong nucleation/reducing agent; therefore, the addition of DPP to the former batches might lead to better results than addition to the latter batches (shown in

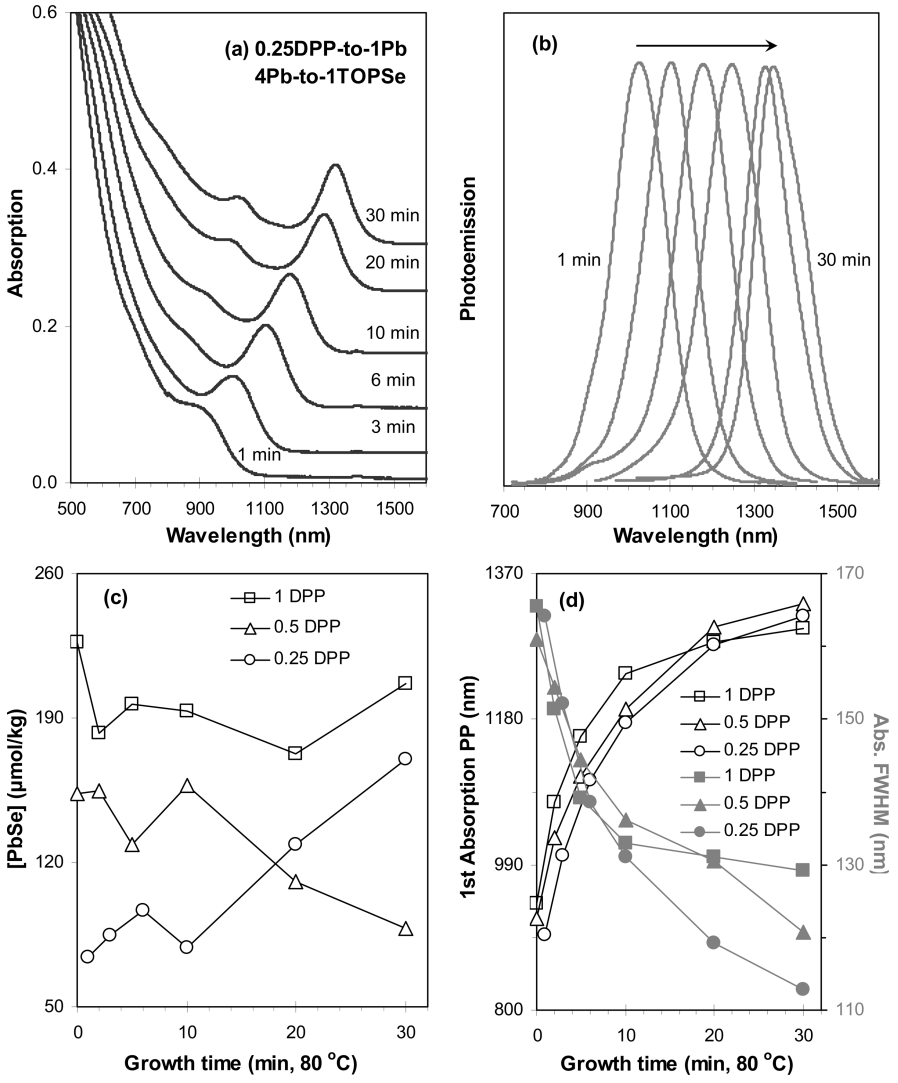

Figure 3. Investigation of the effect of the presence of DPP on the formation of PbSe NCs. The NCs were synthesized from batches with a feed molar ratio of 4:1 Pb-to-TOPSe and [Se] ~ 71 mmol/L. Growth was carried out at 80 °C. (a) Temporal evolution of absorption (offset and normalized to the same height of the excitonic absorption peaks) and (b) PL emission (normalized) of the PbSe NCs with a feed molar ratio of 0.25:1 DPP-to-Pb. (c) [PbSe] in μmol/kg obtained for the PbSe NCs from the three batches with various amounts of DPP: feed molar ratios of (1, 0.5, and 0.25):1 DPP-to-Pb. (d) First excitonic absorption peak positions in nm (left *y* axis) and absorption fwhm in nm (right *y* axis) of the PbSe NCs from the three batches. For PL QY, temporal evolution of the absorption of the NCs from the three batches, and for TEM images, see Figure S3 in the SI.

Figures 2 and S2 in the SI). As mentioned above for method (1), the effect of the TOP amounts is more recognized for syntheses with high Pb-to-TOPSe feed molar ratios. Figure 3 [method (2)] shows the effect of the presence of DPP on the formation of PbSe NCs from the three batches with a feed molar ratio of 4:1 $Pb(OA)_2$-to-TOPSe, [Se] of ~71 mmol/kg, and a growth temperature of 80 °C. The DPP-to-Pb feed molar ratios were (0.25, 0.5, 1):1 DPP-to-Pb. It is worth noting that, as shown by Figure S1B in the SI, nucleation and growth of the PbSe NCs was very difficult for the batch with a 4:1 $Pb(OA)_2$-to-TOPSe feed molar ratio [method (1)]. Strikingly, the addition of DPP [method (2)] could overcome completely such difficulty, leading to the formation of small-sized PbSe NCs with nearly 100% chemical yields and excellent quality. Such an improvement may be argued that DPP greatly enhanced route b shown by eq bM so that formation of the monomer led to balanced nucleation and growth.

With a feed molar ratio of 0.25:1 DPP-to-Pb, the resulting PbSe NCs exhibited a red shift of their absorption peak positions from 898 to 1314 nm (Figure 3a), during growth from 1 to 30 min at 80 °C, and a red shift of their emission peak positions from 1025 to 1362 nm (Figure 3b). The emission fwhm was in the range of ~140−154 nm.

Figure 3c summarizes evolution of [PbSe] during growth from the three synthetic batches with (0.25, 0.5, 1):1 DPP-to-Pb feed molar ratios. For batch 0.25:1 DPP-to-Pb, [PbSe] continuously increased from ~74 to ~170 μmol/kg from 1 to 30 min. The chemical yields at 6, 10, 20, and 30 min were ~33, 35, 73, and 100%, respectively. We highlight our 100% chemical yield reached with the 30-min growth, leading to the PbSe NCs exhibiting their first absorption peak at ~1314 nm and thus ~4.2 nm in size. Without reducing agents added, 100% chemical yield was reported for large PbSe NCs (~9 nm) from reaction at 150 °C with a 1:2 Pb-to-TOPSe feed molar ratio (5). For batch 0.5:1 DPP-to-Pb, an average value of ~150 μmol/kg of [PbSe] was obtained within 10 min of growth. Afterward, [PbSe] continuously decreased to ~109 μmol/kg at 20 min and to ~86 μmol/kg at 30 min. The chemical yields from

5 to 30 min were 45−74%. Here, a decrease of [PbSe] does not imply the occurrence of NC ripening because the absorption fwhm continuously decreased from 154 nm at 2 min to 121 nm at 30 min (see Figure 3d). The emission fwhm was in the range of ∼144−159 nm. For batch 1:1 DPP-to-Pb, an average value of ∼196 μmol/kg of [PbSe] was obtained within 30 min of growth. The chemical yields at 2, 5, and 10 min were ∼59, 85, and 100%, respectively. As shown in Table 1, this 100% chemical yield reached was with the 10-min growth, leading to the PbSe NCs exhibiting their first absorption peak at ∼1239 nm and thus ∼3.9 nm in size. The emission fwhm was in the range of ∼144−161 nm. Therefore, it seemed that [PbSe] increased with an increase of the DPP amount within our experimental conditions. Nucleation and growth was not separated for batch 0.25:1 DPP-to-Pb but was quickly separated for the remaining two batches. Thus, for method (2) with feed molar ratios of 4:1 $Pb(OA)_2$-to-TOPSe and DPP-to-P$b \leq 1$ (where DPP is not excess), the larger the DPP amount used, the more the Pb−P complex (shown in eq bM) formed and the more the nuclei formed.

Figure 3d examines evolution of the absorption peak position and absorption fwhm. The size of the PbSe NCs increased with an increase of the DPP amount except batch 1:1 DPP-to-Pb after the ∼10-min growth, which can be related to the deficiency of the monomer. For the three batches, the absorption fwhm decreased continuously; after the 10-min growth, the absorption fwhm became ∼110−130 nm.

Figure S3A in the SI elucidates evolution of the emission efficiency of the PbSe NCs from the three batches shown in Figure 3. For batch 0.25:1 DPP-to-Pb, the PbSe NCs exhibited the highest PL QY of ∼94% with 20-min growth. For batch 0.5:1 DPP-to-Pb, the highest PL QY was ∼83% also with 20-min growth. For batch 1:1 DPP-to-Pb, the PL QY was ∼50% with 20-min growth. With an increase of the DPP amount, a decrease of the PL QY of the PbSe NCs with growth periods longer than 10 min was worth noting. Within growth periods of 10 min, the PbSe NCs from batch 0.5:1 DPP-to-Pb exhibited the highest PL QY. Again, our experimental results suggested that the presence of DPP could promote the PL QY; such a conclusion, however, is not in agreement with what was documented previously.[25]

Here, the use of DPP, together with the optimized synthetic parameters such as the feed molar ratios of Pb-to-Se, DPP-to-Pb, and OA-to-Pb and the growth temperature, could lead to small-sized PbSe NCs with high particle/chemical yields and high QY, meeting successfully the requirement of the sizable nucleation at low temperature with consumption of a large amount of the monomer. Thus, the quality of the resulting PbSe NCs, including the size, size distribution, and emission brightness, is highly related to control of the experimental conditions for formation of the monomer and thus for balanced nucleation and growth. The narrow size distribution and high crystallinity of the resulting PbSe NCs were evidenced by TEM (see Figure S3C in the SI).

Figure 4 shows the effect of the presence of TBP on the growth of PbSe NCs when TOPSe/TOP was used as the Se precursor [method (3)]. For the four batches studied, the feed molar ratio was 1:2.5 Pb-to-Se, together with [Pb] ∼ 71 mmol/L and a growth temperature of 80 °C. Different amounts of TBP were added directly into the reaction at ∼30−35 °C. To minimize the solvency effect, the TBP amount was kept below ∼11% (v/v). The absorption spectra of the PbSe NCs from the four batches are presented in Figure S4 in the SI. As shown by Figures 4 and S4 in the SI and Table 1, the larger the TBP amount, the higher the particle number achieved. The particle concentrations of the 35-min growth samples from batches (0, 0.6, 1.2, and 1.6):1 TBP-to-Pb were ∼2.6, 7.3, 9.3,

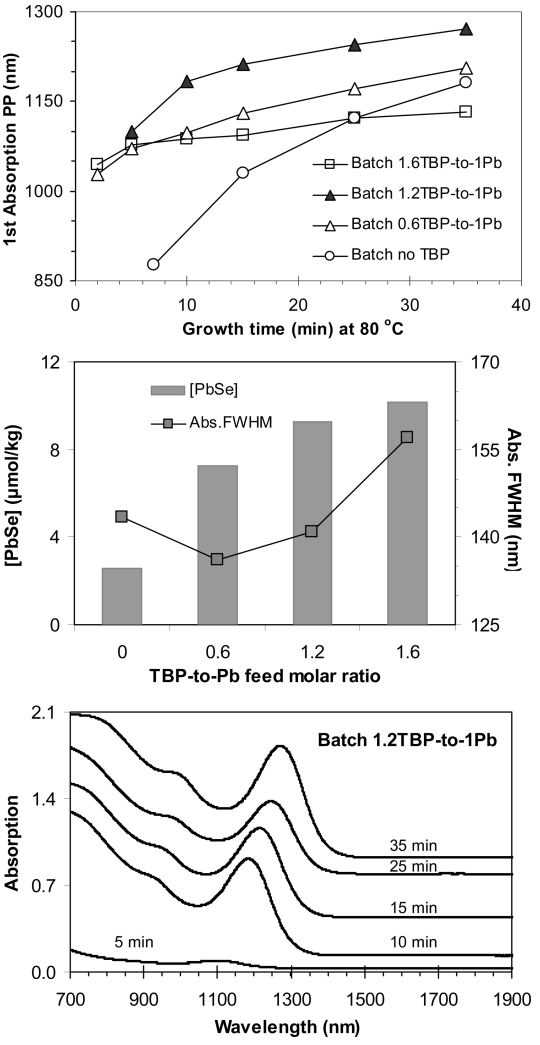

Figure 4. Investigation on the effect of TBP added on the formation of PbSe NCs. The NCs were synthesized from the four batches with a feed molar ratio of 1:2.5 Pb-to-TOPSe and [Pb] of ∼71 mmol/L. The volume of the reaction medium of each batch was ∼8 mL; the amounts of TBP added are indicated as the TBP-to-Pb feed molar ratios. The growth temperature was ∼80 °C. (Top) First excitonic absorption peak positions of the NCs from the four batches. (Middle) [PbSe] in μmol/kg in the growth mixtures (left *y* axis) and the absorption fwhm in nm (right *y* axis) of the 35-min growth samples from the four batches. (Bottom) Temporal evolution of absorption (offset) of the PbSe NCs from batch 1.2:1 TBP-to-Pb [7.6% (v/v)]. The absorption spectra were normalized to 1.0 g of crude growth mixtures and dispersed in 1.0 mL of TCE.

and 10.1 μmol/kg, while the chemical yields were ∼1.1%, 3.3%, 5.1%, and 3.7%, respectively. Note that the size of the 35-min ensemble of batch 1.6:1 TBP-to-Pb is smaller than that of batch 1.2:1 TBP-to-Pb. Thus, with the 35-min growth, batch 1.6:1 TBP-to-Pb exhibited a higher particle concentration but a lower chemical yield than batch 1.2:1 TBP-to-Pb. Accordingly, the degree of the reactions could be featured more precisely by particle yields [PbSe] than chemical/conversion yields; the former is size-independent, but the latter is size-dependent. The resulting PbSe NCs maintained a narrow size distribution with their absorption fwhm values of ∼135−155 nm. It seems reasonable that, in our noninjection approach, TBP promoted formation of the PbSe monomer and thus enhanced the size/degree of nucleation, leading to a ∼3-fold increase of [PbSe] [compared to method (1)]. Here, DBP and TBP

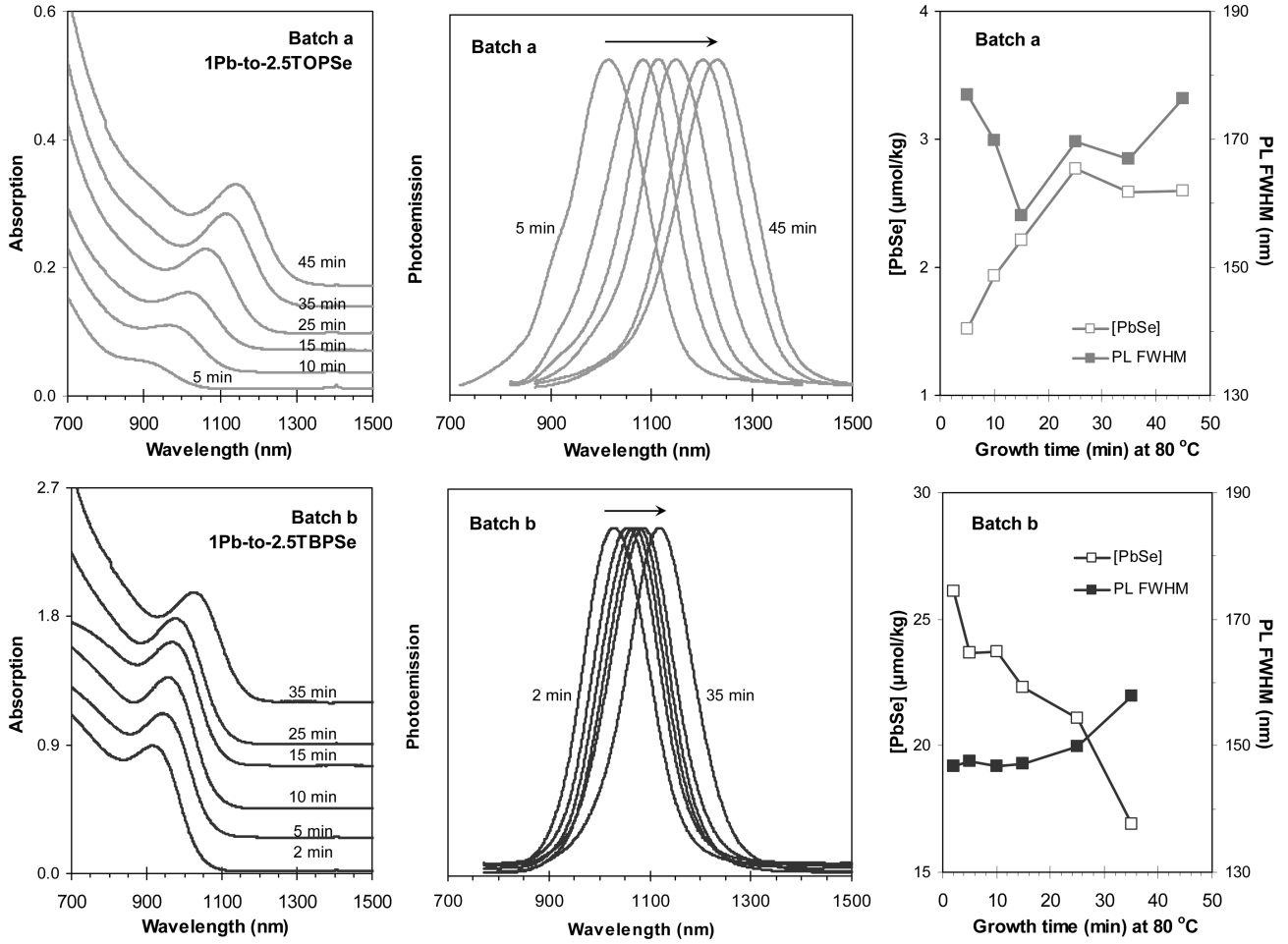

Figure 5. Comparison of the effect of TOPSe and TBPSe on the formation of PbSe NCs. The NCs were synthesized from the two batches with feed molar ratios of 1:2.5 Pb-to-TOPSe (batch a) and 1:2.5 Pb-to-TBPSe (batch b) and [Pb] of ~71 mmol/L. (Left) Temporal evolution of absorption (offset), (middle) temporal evolution of emission (normalized), and (right) [PbSe] in μmol/kg in the growth mixtures (left y axis) and PL fwhm in nm (right y axis). The growth temperature was 80 °C, and the growth periods are indicated. The absorption spectra were normalized to 1.0 g of crude reaction mixtures in 1.0 mL of TCE. Diluted sample dispersions in TCE were used for the emission measurements with absorbance at the excitation wavelength of ~0.1. The excitation wavelength for batch a was 700 nm for the 5-min sample, 800 nm for the 10- and 15-min samples, and 850 nm for the 25-, 35-, and 45-min samples, while 750 nm was used for all of the samples from batch b.

acted as nucleation agents,[25,30] forming Pb−P complexes with $Pb(oleate)_2$ and thus enhancing route b (eq bM), resulting in the formation of more nuclei at ~65 °C. With the presence of 10.6% TBP (batch 1.6:1 TBP-to-Pb), the growth was very tight; such a slow growth could be attributed to a low monomer concentration available after formation of a large number of nuclei.

Now, let us compare the effects of DOPSe/TOPSe [method (1)] and DBPSe/TBPSe [method (4)]. Figure 5 shows the temporal evolution of optical properties of the growing PbSe NCs from two batches with DOPSe/TOPSe (a) and DBPSe/TBPSe (b) as the Se precursor (the molar ratio was 1:2.2 Se-to-TOP/TBP). The other conditions were identical: a feed molar ratio of 1:2.5 Pb-to-Se, [Pb] of ~71 mmol/L, and a growth temperature of 80 °C.

For the TOPSe batch (batch a), nucleation seemed to take place at ~80 °C. [PbSe] increased continuously from ~1.5 μmol/kg (at 5 min) to ~2.8 μmol/kg (at 25 min), indicating a continuous nucleation and the absence of complete separation of the nucleation and growth periods. From 25 to 45 min, an average value of ~2.6 μmol/kg of [PbSe] was obtained, with an average chemical yield of ~0.9%. The PL QY was in the range of ~30−50%.

For the TBPSe batch (batch b), nucleation seemed to occur at ~50 °C. Note that this nucleation temperature is lower than that observed in the TOPSe systems with TBP addition (~65 °C as shown in Figure 4) and the TOP system (as shown in Figures 1 and 5, top). A tighter growth was observed, and the resulting PbSe NCs exhibited narrower absorption and emission fwhm, suggesting narrower size distribution. An average value of ~22.7 μmol/kg of [PbSe] was obtained (from 5 to 25 min), which is an ~8-fold increase compared to that obtained from the TOPSe system. The PL QY was in the range of ~70−90%. Here, nucleation was fast and sizable, leading to the formation of a large number of nuclei/nanocrystals in a short time and a speedy depletion of the monomer; therefore, the leisurely growth in the size was monitored. At 35 min, [PbSe] was ~16.9 μmol/kg and the chemical yield was ~4.3%, as shown in Table 1. Thus, after 25 min, the severe decrease in [PbSe], together with the significant broadening in the absorption fwhm, indicates the presence of ripening (due to shortage of the monomer). Detailed investigation and discussion on the synthetic parameters, such as $Pb(OA)_2$-to-TBPSe feed molar ratios, the amount of oleic acid used, and the reaction temperature, are presented in Figure S5 in the SI.[33,39]

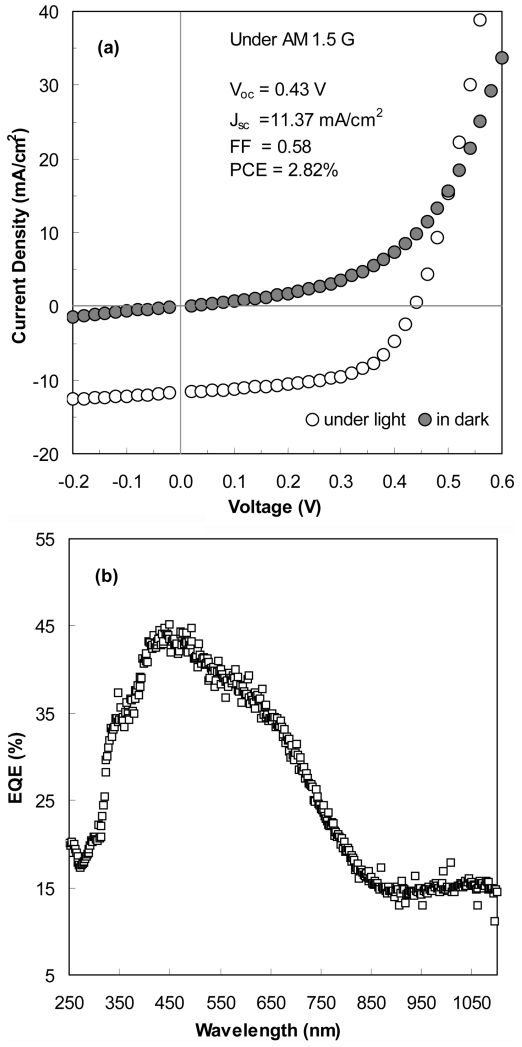

Figure 6. (a) Current density−voltage ($J-V$) characteristics of a PbSe NC-based Schottky-type solar cell under AM 1.5G irradiation of 100 mW/cm^2. The first excitonic absorption peak of the PbSe NCs is at 1131 nm. The device parameters listed in the inset were extracted from the $J-V$ curve except J_{sc} and PCE, which were calibrated values using the EQE data. (b) EQE spectrum of the solar cell.

Our small-sized PbSe NCs have exhibited excellent storage stability (see Figure S6A in the SI for diluted TCE dispersions and Figure S6B in the SI for concentrated TCE dispersions). For the diluted dispersions, the absorption peaks of the PbSe NCs from the four batches blue-shifted over time; however, the corresponding emission intensity was almost maintained, or even enhanced, during 3 months of storage in a freezer (in the dark at −20 °C). For the concentrated dispersions, the PbSe NCs from the optimized batches studied (Figure S5 in the SI) have also demonstrated superior stability. For example, the recommended batches are with a feed molar ratio of 2:1 Pb-to-Se, 60 °C growth temperature, and a feed molar ratio of 3.3:1 OA-to-Pb. The PbSe NCs exhibited only a 3-nm blue shift, a 10-nm blue shift, and a 8-nm red shift of their first excitonic absorption peaks after ∼3.5 months of storage in a freezer (in the dark at −20 °C) and possessed ∼59%, ∼64%, and ∼98% PL QY, respectively (as shown in Figure S6B and Table S2 in the SI). When the blue shifts were the smallest, the corresponding PL QYs were the highest, as compared in the same group shown in Figures S5, S5A, and S5B in the SI, showing the effect of the synthetic parameters on formation of the PbSe NCs. Such excellent stability is worth noting. The poor storage stability at room temperature of the dispersions of large-sized PbSe NCs in TCE was documented: the blue shift of the band-gap absorption, together with the significant and monotonous decrease of the corresponding band-gap emission.[40] Such instability was ascribed to photooxidation.[40−43]

Our PbSe NC prepared from the noninjection-based approach is a cubic rock salt of crystal structure (Figure S7A in the SI). The high synthetic reproducibility is also demonstrated and is worth noting (Figure S7B in the SI). Furthermore, our small-sized PbSe NCs are Pb-rich on the surface, and the Pb/Se atomic ratio decreases as the size increases (Figure S7C in the SI).

Therefore, our small-sized PbSe NCs with high particle yield are high quality, in terms of their optical properties with high QY and narrow bandwidth, together with their stability. Furthermore, these small-sized PbSe NCs have demonstrated their potential in PV applications. For example, a Schottky-type solar cell made of PbSe NCs, with their first excitonic absorption peaking at 1131 nm, exhibited a PCE value of 2.82%. This is the highest PCE value reported from the same type of devices. Figure 6 shows the current density−voltage ($J-V$) curve of this cell under AM 1.5G irradiation of 100 mW/cm^2 and the external quantum efficiency (EQE) spectrum. The inset lists the PV parameters extracted from the $J-V$ curve. It is worth noting that the J_{sc} and PCE listed are the calibrated data using the EQE spectrum. As can be seen, the EQE spectrum shows a broad response covering 250−1100 nm, with the first excitonic peak observable at about 1100 nm, which is consistent with the absorption spectrum. The device has very good V_{oc} (0.43 V) and FF (0.58), among the best data reported for PbSe NC Schottky-type solar cells. The high V_{oc} can be attributed to the relatively large band gap of our PbSe NCs ($E_g \approx 1.1$ eV) because the open-circuit voltage of PbSe NC Schottky-type solar cells has been shown to be dependent linearly on the band gap of the NCs.[12,14] The high FF suggests a limited loss from charge recombination, which is important for efficient charge transport.

CONCLUSION

We have developed a low-temperature noninjection-based one-pot approach to produce small-sized PbSe NCs with high particle yield, high quality, and high synthetic reproducibility, meeting PV technology demands. The small-sized PbSe NCs are those with their first excitonic absorption of wavelength shorter than 1200 nm. The high quality is in terms of the size distribution, optical properties, and stability. The realization of the formation of such small-sized PbSe NCs with high reaction/chemical/conversion yield, via our low-temperature noninjection one-pot protocol, was achieved by the five methods, including the use of DPP as a nucleation agent. The addition of DPP should have led to formation of a Pb−P complex and thus a large degree and rate of supersaturation of the monomer at low temperature. Subsequently, nucleation took place at low temperature with a large number of nuclei. The PbSe NC concentration could be increased ∼3-fold with the addition of TBP into the reaction with TOPSe as the precursor, ∼8-fold with TBPSe as the precursor instead of TOPSe, and ∼40−50-fold (or ∼4-fold) with the use of DPP and with TOPSe (or TBPSe) as the precursor. The corresponding chemical yields were ∼1−2% with TOPSe as the precursor and without reducing agents added

[method (1)], ∼4−5% with the addition of TBP [method (3)] or TBPSe as the Se precursor [method (4)], ∼30−40% with the addition of DPP [method (5), with a 1:2.5 Pb-to-TBPSe feed molar ratio], and ∼70−100% with the addition of DPP [method (2), with a 4:1 Pb-to-Se feed molar ratio]. With the presence of DPP, the large optimal window of the Pb-to-Se feed molar ratio leading to small-sized PbSe NCs with high yield and high quality is worth noting, such as a 4:1 Pb-to-Se feed molar ratio. A mechanism was proposed for low-temperature formation of the PbSe monomer, involving Pb−Se (route aM) and Pb−P (route bM) complexes. Our experimental batches with methods (1) and (2) suggest that route b (eq bM) was dominant for method (2), while route a was dominant for method (1). Our small-sized PbSe NCs produced were high quality, exhibiting narrow absorption and emission (with PL fwhm ∼130−150 nm) and high PL QY ∼50−90%. With an understanding of the monomer formation mechanism and its guidance on promotion of the reactivity of the Pb−Se and Pb−P complexes leading to sizable nucleation at low temperature, our study demonstrates that the synthetic parameters must be tuned carefully in order to achieve high reactivity of the complexes for balanced nucleation/growth for small-sized NCs with high yield and high quality. Our thorough exploration on the PbSe low-temperature syntheses brings insight to the monomer formation mechanism and the controlled synthesis of small-sized NCs with high reaction yield and quality and, thus, should have an impact on colloidal science and the development of next-generation low-cost and high-efficiency solar cells. Our small-sized PbSe NCs have demonstrated very promising results in our preliminary PV device testing, with high V_{oc}, good FF, and a record-breaking PCE (2.82%). Finally, the mechanism proposed for PbSe monomer formation at low temperature should be suitable to other QD systems such as IV−VI, II−V, and II−VI; furthermore, route b could be promoted by various chemicals including phosphines, diols, and amines. Low-cost and environmentally friendly chemicals could be considered. Thus, the present synthetic study represents an important step toward how to design and synthesize desired QDs via control of the two active routes, leading to formation of the monomer and thus sizable nucleation at low temperature. This mechanism offers a promising low-temperature approach to reproducible syntheses of high-quality NCs with high yields.

EXPERIMENTAL METHODS

All chemicals used are commercially available from Sigma-Aldrich (or otherwise specified) and were used as received: PbO (99.999%), oleic acid (OA; tech. 90%), 1-octadecene (ODE; tech. 90%), selenium (Se; ∼200 mesh, 99.999%, Alfa Aeser), *n*-trioctylphosphine (TOP; tech. 90%), *n*-tributylphosphine (TBP; 97%), diphenylphosphine (DPP; 98%), tetrachloroethylene (TCE; ≥ 99%, spectrophotometric grade), 1,2-dichloroethane (≥99%, spectrophotometric grade), and dye IR 26 (Exciton). The solvents used for purification were toluene (99.5%, ACS reagent, ACP in Montreal), hexane (98.5%, GR ACS, EMD in USA), methanol (absolute, ACP in Montreal), and acetone (99.5%, ACS reagent, ACP in Montreal).

Standard air-free techniques were used throughout all syntheses. To make a $Pb(oleate)_2$ stock solution of 0.681 mmol/g, 6.0085 g (26.92 mmol) of PbO, 17.028 g (60.19 mmol, without consideration of 90% purity) of OA, 16.976 g of ODE were placed in a three-neck, 100-mL round-bottomed flask equipped with an air condenser and a thermocouple; the mixture was degassed under vacuum at room temperature until there was no vigorous bubbling and then heated to ∼180 °C under purified nitrogen until all PbO was dissolved and a clear solution was obtained, followed by degassing (∼50 mtorr) at ∼110 °C for 1 h.

To make a TOPSe/TOP stock solution of 1.09 M, 3.2725 g (41.45 mmol) of Se powder and 34.628 g (93.43 mmol, without the consideration of 90% purity) of TOP were added to a 100-mL Schlenk flask. The mixture was then degassed under vacuum at room temperature until bubbling ceased, followed by gentle heating under purified nitrogen until a clear solution was obtained. To make a TBPSe/TBP stock solution of 1.80 M, 1.4250 g (18.05 mmol) of Se powder was sonicated in 10.0 mL (40.04 mmol, without the consideration of 97% purity) of TBP for ∼30 min until a clear solution was obtained; the TBPSe stock solution was kept in a glovebox with a nitrogen atmosphere.

In a typical synthesis of PbSe NCs via our one-pot noninjection-based synthetic protocol, 0.845 g (0.58 mmol) of a $Pb(oleate)_2$ stock solution, 1.346 g (1.47 mmol of Se) of a TOPSe/TOP stock solution, and 4.401 g of ODE were mixed in a three-neck, 50-mL round-bottomed flask equipped with an air condenser and a thermometer. The mixture was degassed under vacuum and then purged with purified nitrogen at least three times in 30 min at 30−35 °C. Afterward, the mixture was heated under purified nitrogen to a desired temperature such as 80 °C with a heating rate of ∼10 °C/min. Therefore, such a batch had feed molar ratios of 2.2:1 OA-to-Pb and 1:2.5 Pb-to-Se and [Pb] of ∼71 mmol/L in a ∼8-mL reaction medium. For those syntheses with TBPSe/TBP instead of TOPSe/TOP, 0.82 mL of a TBPSe/TBP stock solution (containing 1.48 mmol of Se) and ∼5.0 g of ODE was used. Usually, the total reaction volume was kept at ∼8 mL via adjustment of the ODE amount, while the reactant concentration was maintained at ∼71 mmol/L. To examine the effect of the presence of a reducing agent of TBP or DPP, a certain amount of TBP or DPP was added to a reaction flask right before an increase in the temperature.

To monitor the growth kinetics, small aliquots (∼1 g) were quickly taken out of the reaction flask. Each sample was weighed, then dispersed in toluene, precipitated with methanol, and centrifuged. The precipitates were dispersed again in toluene, precipitated with methanol, and centrifuged. Afterward, the precipitates were further dispersed in hexane and precipitated with acetone (if needed, a small amount of methanol was added to cause the complete precipitation of the NCs). The purified samples were dried by a fast flow of nitrogen and then dispersed in 1.0 mL of TCE. To minimize any possible change of the NCs, optical measurements were carried out immediately for the purified samples dispersed in 1.0 mL of TCE.

Ultraviolet−visible−near-IR (UV−vis−NIR) absorption spectra were collected using a 1-nm data interval (Varian Cary 5000 spectrophotometer). Quantitative dilution was performed when the sample dispersion was too concentrated. Gaussian fitting was conducted using Pro Origin 8 to yield the first excitonic absorption peak position, fwhm, and height. Using Lambert−Beer's law, $A = \varepsilon CL$, the nanocrystal molar concentration, C, was calculated, where ε, the molar extinction coefficient, was estimated from the PbSe size and corrected by size distribution.[26] The nanocrystal concentration, [PbSe], in the reaction mixture was back-calculated based on the weight of the aliquots taken. There is another method to get ε, where $\varepsilon_{3.1\ eV}$ is also size-dependent but irrespective of size distribution.[43] The two methods are in agreement with each other in ε values.[44]

Near-IR PL emission spectra were collected with a Horiba Jobin Yvon Fluorolog-3 model FL3-11 spectrofluorometer, equipped with a 2-mm-diameter InGaAs photodiode whose operating temperature was at −196 °C with the working range of 1000−1500 nm. Both the entrance and exit slits were 3 nm, and the data increment was 1 nm. Dilute PbSe NC dispersions in TCE were used, with ∼0.1 optical density at the excitation wavelength used. Origin 8 was used for integration with baseline subtraction and Gaussian fitting, in order to obtain information on the emission peak position, fwhm, and area (intensity). The PL QY was estimated by comparing the sample emission intensity with that of IR26 dye in dichloroethane (lit. QY 0.5%).[38]

Corrections were made for the difference of the refractive index of the two solvents and for the detector response sensitivity. Recently, a different value of IR26 QY was reported,[45] compared to that used before.[5,6,38,42]

The TEM samples were prepared by depositing dilute purified NC dispersions in TCE or hexane onto 400-mesh thin-carbon-coated copper grids, together with air-drying. TEM images were collected on a JEOL JEM-2100F electron microscope operating at 200 kV and equipped with a Gatan UltraScan 1000 CCD camera. The NC size and standard deviation were obtained by analyzing ~500−900 individual PbSe NCs with the Gatan Digital Micrograph built-in statistics function.

The potential of our small-sized PbSe NCs in solar cell application has been examined using a Schottky-type diode configuration, with a structure of indium tin oxide (ITO)/PbSe NCs/LiF (1 nm)/Al (100 nm). Prepatterned ITO-coated glass substrates were cleaned stepwise by an ultrasonic bath in acetone and isopropyl alcohol and then treated by UV ozone for 15 min right before use. The active layers were cast using a sequential layer-by-layer cross-linking technique. First, a 5-mg/mL solution of as-synthesized PbSe NCs in hexane was spin-cast on top of the ITO substrate at 5000 rpm to form a 7−9-nm-thick film, corresponding to 1−2 monolayers of the NCs. After the NC layer was cast, the substrate was soaked in 0.02 M 1,3-benzenedithiol in acetonitrile for 30 s and then immediately removed from the solution and spun at 5000 rpm for 1 min to quickly dry the film. A desired film thickness was achieved by repeating this process. Finally, a LiF/Al electrode was thermally evaporated on top of the NC film to serve as the cathode. The resulting devices have an active area of 0.09 cm^2. Both the film preparation and device testing were done in gloveboxes filled with dry nitrogen. The $J-V$ characteristics were measured with a Keithley 2400 sourcemeter under one sun of simulated air mass 1.5G (AM 1.5G) solar irradiation of 100 mW/cm^2. The EQE data were acquired with a customer made setup consisting of a Jobin-Yvon Triax 180 spectrometer, a Jobin-Yvon xenon light source, a Merlin lock-in amplifier, a calibrated Si detector, and a SR 570 low-noise current amplifier.

■ ASSOCIATED CONTENT

Supporting Information. ^{31}P NMR spectrum showing no detectable DPPSe formation from TOPSe and DPP, TEM of our scaled-up synthesis via a one-pot noninjection approach, effect of the Pb-to-TOPSe feed molar ratio on the noninjection synthesis of PbSe NCs, TOP amount effect, effect of the Pb-to-Se feed molar ratio, growth temperature, and OA-to-Pb feed molar ratio on the formation of PbSe NCs with TBPSe as the precursor and the storage stability of the resulting NCs, effect of the DPP amount on the formation of the PbSe NCs with TOPSe as the precursor, the storage stability of our small-sized PbSe NCs synthesized with TOPSe and TBPSe (with and without the presence of DPP), typical TEM images of the small-sized PbSe NCs, and powder X-ray diffraction pattern indicating the cubic rock-salt crystal structure of the PbSe NCs from the noninjection-based approach. This material is available free of charge via the Internet at http://pubs.acs.org.

■ AUTHOR INFORMATION

Corresponding Author

*Phone: 1-(613)-993-9273. E-mail: kui.yu@nrc.ca.

■ ACKNOWLEDGMENT

J.O. is thankful for a NRC−NSERC−BDC grant for financial support. We thank Dr. Hsien-Tse Tung for his assistance in some syntheses and discussion, Dr. Dennis Whitfield for a discussion on the monomer formation mechanism, and Dr. Sai-Wing Tsang for his assistance in some device measurements and discussion. We thank Wenhui Hao for use of the instrument for some emission measurements in Carleton University.

■ REFERENCES

(1) Sargent, E. H. *Adv. Mater.* **2005**, *17*, 515–522.
(2) Wise, F. W. *Acc. Chem. Res.* **2000**, *33*, 773–780.
(3) Murray, C. B.; Sun, S.; Gaschler, W.; Doyle, H.; Betley, T. A.; Kagan, C. R. *IBM J. Res. Dev.* **2001**, *45*, 47–56.
(4) Du, H.; Chen, C.; Krishnan, R.; Krauss, T. D.; Harbold, J. M.; Wise, F. W.; Thomas, G.; Silcox, J. *Nano Lett.* **2002**, *2*, 1321–1324.
(5) Yu, W. W.; Falkner, J. C.; Shih, B. S.; Colvin, V. L. *Chem. Mater.* **2004**, *16*, 3318–3322.
(6) Pietryga, J. M.; Schaller, R. D.; Werder, D.; Stewart, M. H.; Klimov, V. I.; Hollingsworth, J. A. *J. Am. Chem. Soc.* **2004**, *126*, 11752–11753.
(7) Murphy, J. E.; Beard, M. C.; Norman, A. G.; Ahrenkiel, S. P.; Johnson, J. C.; Yu, P. R.; Micic, O. I.; Ellingson, R. J.; Nozik, A. J. *J. Am. Chem. Soc.* **2006**, *128*, 3241–3247.
(8) Evans, C. M.; Guo, L.; Peterson, J. J.; Maccagnano-Zacher, S.; Krauss, T. D. *Nano Lett.* **2008**, *8*, 2896–2899.
(9) Medintz, I. L.; Uyeda, H. T.; Goldman, E. R.; Mattoussi, H. *Nat. Mater.* **2005**, *4*, 435–446.
(10) Resch-Genger, U.; Grabolle, M.; Cavaliere-Jaricot, S.; Nitschke, R.; Nann, T. *Nat. Methods.* **2008**, *5*, 763–775.
(11) Koleilat, G. I.; Levina, L.; Shukla, H.; Myrskog, S. H.; Hinds, S.; Pattantyus-Abraham, A. G.; Sargent, E. H. *ACS Nano* **2008**, *2*, 833–840.
(12) Luther, J. M.; Law, M.; Beard, M. C.; Song, Q.; Reese, M. O.; Ellingson, R. J.; Nozik, A. J. *Nano Lett.* **2008**, *8*, 3488–3492.
(13) Law, M.; Beard, M. C.; Choi, S.; Luther, J. M.; Hanna, M. C.; Nozik, A. J. *Nano Lett.* **2008**, *8*, 3904–3910.
(14) Choi, J. J.; Lim, Y.-F.; Santiago-Berrios, M. B.; Oh, M.; Hyun, B.-R.; Sun, L.; Bartnik, A. C.; Goedhart, A.; Malliaras, G. G.; Abruña, H. D.; Wise, F. W.; Hanrath, T. *Nano Lett.* **2009**, *9*, 3749–3755.
(15) Hillhouse, H. W.; Beard, M. C. *Curr. Opin. Colloid Interface Sci.* **2009**, *14*, 245–259.
(16) Buhl, M. L., Jr.; Bird, R. E.; Bilchak, R. V.; Connolly, J. S.; Bolton, J. R. *Solar Energy* **1984**, *32*, 75–84.
(17) Steckel, J. S.; Coe-Sullivan, S.; Bulović, V.; Bawendy, M. G. *Adv. Mater.* **2003**, *15*, 1862–1866.
(18) Finlayson, C. E.; Sazio, P. J. A.; Sanchez-Martin, R.; Bradley, M.; Kelf, T. A.; Baumberg, J. J. *Semicond. Sci. Technol.* **2006**, *21*, L21–L24.
(19) Cheng, C.; Zhang, H. *Opt. Commun.* **2007**, *277*, 372–378.
(20) Ellingson, R. J.; Beard, M. C.; Johnson, J. C.; Yu, P.; Micic, O. I.; Nozik, A. J.; Shabaev, A.; Efros, A. L. *Nano Lett.* **2005**, *5*, 865–871.
(21) Schaller, R. D.; Sykora, M.; Pietryga, J. M.; Klimov, V. I. *Nano Lett.* **2006**, *6*, 424–429.
(22) Nozik, A. J. *Chem. Phys. Lett.* **2008**, *457*, 3–11.
(23) Ji, M.; Park, S.; Connor, S. T.; Mokari, T.; Cui, Y.; Gaffney, K. J. *Nano Lett.* **2009**, *9*, 1217–1222.
(24) Shockley, W.; Queisser, H. J. *J. Appl. Phys.* **1961**, *32*, 510–519.
(25) Joo, J.; Pietryga, J. M.; McGuire, J. A.; Jeon, S.-H.; Williams, D. J.; Wang, H.-L.; Klimov, V. I. A *J. Am. Chem. Soc.* **2009**, *131*, 10620–10628.
(26) Dai, Q.; Wang, Y.; Li, X.; Zhang, Y.; Pellegrino, D. J.; Zhao, M.; Zou, B.; Seo, J. T.; Wang, Y.; Yu, W. W. *ACS Nano* **2009**, *3*, 1518–1524.
(27) Ouyang, J.; Zaman, B.; Yan, F.; Johnston, D.; Li, G.; Wu, X.; Leek, M. D.; Ratcliffe, C. I.; Ripmeester, J. A.; Yu, K. *J. Phys. Chem. C* **2008**, *112*, 13805–13811.
(28) Wang, R.; Ouyang, J.; Nikolaus, S.; Brestaz, L.; Zaman, Md. B.; Wu, X.; Leek, M. D.; Ratcliffe, C. I.; Yu, K. *Chem. Commun.* **2009**, 962–964.
(29) Li, M.; Ouyang, J.; Ratcliffe, C. I.; Pietri, L.; Wu, X.; Leek, D. M.; Moudrakovski, I.; Lin, Q.; Yang, B.; Yu, K. *ACS Nano* **2009**, *3*, 3832–3838.

(30) Steckel, J. S.; Yen, B. K. H.; Oertel, D. C.; Bawendi, M. G. *J. Am. Chem. Soc.* **2006**, *128*, 13032–13033.
(31) Evans, C. M.; Evans, M. E.; Krauss, T. D. *J. Am. Chem. Soc.* **2010**, *132*, 10973–10975.
(32) Liu, T.-Y.; Li, M.; Ouyang, J.; Zaman, Md. B.; Wang, R.; Wu, X.; Yeh, C.-S.; Lin, Q.; Yang, B.; Yu, K. *J. Phys. Chem. C* **2009**, *113*, 2301–2308.
(33) Ouyang, J.; Kuijper, J.; Brot, S.; Kingston, D.; Wu, X.; Leek, D. M.; Hu, M. Z.; Yu, K. *J. Phys. Chem. C* **2009**, *113*, 7579–7593.
(34) Ouyang, J.; Ratcliffe, C. I.; Kingston, D.; Wilkinson, B.; Kuijper, J.; Wu, X.; Ripmeester, J. A.; Yu, K. *J. Phys. Chem. C* **2008**, *112*, 4908–4919.
(35) Yu, K.; Ouyang, J.; Zaman, B.; Johnston, D.; Yan, F.; Li, G.; Ratcliffe, C. I.; Leek, M. D.; Wu, X.; Stupak, J.; et al. *J. Phys. Chem. C* **2009**, *113*, 3390–3401.
(36) Wang, R.; Ratcliffe, C. I.; Wu, X.; Voznyy, O.; Tao, Y.; Yu, K. *J. Phys. Chem. C* **2009**, *113*, 17979–17982.
(37) Yu, K.; Hu, M. Z.; Wang, R.; Piolet, M.; Frotey, M.; Zaman, Md. B.; Wu, X.; Leek, D. M.; Tao, Y.; Wilkinson, D.; Li, C. *J. Phys. Chem. C* **2010**, *114*, 3329–3339.
(38) Wehrenberg, B. L.; Wang, C.; Guyot-Sionnest, P. *J. Phys. Chem. B* **2002**, *106*, 10634–10640.
(39) Yu, W. W.; Peng, X. *Angew. Chem., Int. Ed.* **2002**, *41*, 2368–2371.
(40) Dai, Q.; Wang, Y.; Zhang, Y.; Li, X.; Li, R.; Zou, B.; Seo, J. T.; Wang, Y.; Liu, M.; Yu, W. W. *Langmuir* **2009**, *25*, 12320–12324.
(41) Moreels, I.; Fritzinger, B.; Martins, J. C.; Hens, Z. *J. Am. Chem. Soc.* **2008**, *130*, 15081–15086.
(42) Sykora, M.; Koposov, A. Y.; McGuire, J. A.; Schulze, R. K.; Tretiak, O.; Pietryga, J. M.; Klimov, V. I. *ACS Nano* **2010**, *4*, 2021–2034.
(43) Moreels, I.; Lambert, K.; Muynck, D.; Vanhaecke, F.; Poelman, D.; Martins, J. C.; Allan, G.; Hens, Z. *Chem. Mater.* **2007**, *19*, 6101–6106.
(44) Moreels, I.; Lambert, K.; Muynck, D.; Vanhaecke, F.; Poelman, D.; Martins, J. C.; Allan, G.; Hens, Z. *ACS Nano* **2009**, *3*, 2053.
(45) Semonin, O. E.; Johnson, J. C.; Luther, J. M.; Midgett, A. G.; Nozik, A. J.; Beard, M. C. *J. Phys. Chem. Lett.* **2010**, *1*, 2445–2450.

NOTE ADDED AFTER ASAP PUBLICATION

This paper was published on the Web on January 18, 2011, and the original version of the Supporting Information contained an incorrect value in Scheme S1. The corrected version was reposted on February 3, 2011.